

# Optical Recording Reveals Novel Properties of GSK1016790A-Induced Vanilloid Transient Receptor Potential Channel TRPV4 Activity in Primary Human Endothelial Cells<sup>[S]</sup>

Michelle N. Sullivan, Michael Francis, Natalie L. Pitts, Mark S. Taylor, and Scott Earley

*Vascular Physiology Research Group, Department of Biomedical Sciences (M.N.S., N.L.P., S.E.) and Department of Biology, Colorado State University, Fort Collins, Colorado (N.L.P.); and Department of Physiology, University of South Alabama College of Medicine, Mobile, Alabama (M.F., M.S.T.)*

Received March 7, 2012; accepted June 11, 2012

## ABSTRACT

Critical functions of the vascular endothelium are regulated by changes in intracellular  $[Ca^{2+}]$ . Endothelial dysfunction is tightly associated with cardiovascular disease, and improved understanding of  $Ca^{2+}$  entry pathways in these cells will have a significant impact on human health. However, much about  $Ca^{2+}$  influx channels in endothelial cells remains unknown because they are difficult to study using conventional patch-clamp electrophysiology. Here we describe a novel, highly efficient method for recording and analyzing  $Ca^{2+}$ -permeable channel activity in primary human endothelial cells using a unique combination of total internal reflection fluorescence microscopy (TIRFM), custom software-based detection, and selective pharmacology. Our findings indicate that activity of the

vanilloid (V) transient receptor potential (TRP) channel TRPV4 can be rapidly recorded and characterized at the single-channel level using this method, providing novel insight into channel function. Using this method, we show that although TRPV4 protein is evenly distributed throughout the plasma membrane, most channels are silent even during maximal stimulation with the potent TRPV4 agonist *N*-((1*S*)-1-[[4-((2*S*)-2-[[2,4-dichlorophenyl)sulfonyl]amino]-3-hydroxypropanoyl)-1-piperazinyl]carbonyl]-3-methylbutyl)-1-benzothio-*phene*-2-carboxamide (GSK1016790A). Furthermore, our findings indicate that GSK1016790A acts by recruiting previously inactive channels, rather than through increasing elevation of basal activity.

## Introduction

Mechanisms controlling endothelial cell  $Ca^{2+}$  entry, removal, and dynamic release from and reuptake to intracellular stores play a central role in the regulation of vascular tone. For example, a rise in endothelial cell intracellular  $[Ca^{2+}]$  generates nitric oxide by increasing the activity of endothelial nitric-oxide synthase and elevates the activity of phospholipase  $A_2$ , an enzyme that liberates arachidonic acid from the plasma membrane to provide

substrate for the production of potent vasoactive factors (Vanhoutte, 2004). In addition,  $Ca^{2+}$ -activated  $K^+$  channels are directly stimulated by a rise in intracellular  $[Ca^{2+}]$ , leading to hyperpolarization of the membranes of both endothelial cells and electrically coupled vascular smooth muscle cells to elicit vasodilation (Whorton et al., 1984; Taylor et al., 2003; Köhler and Hoyer, 2007). Because endothelial dysfunction is strongly correlated with common cardiovascular diseases, such as hypertension, stroke, and atherosclerosis, new technologies that advance our understanding of  $Ca^{2+}$  movement in these cells will have considerable clinical impact.  $Ca^{2+}$  influx via members of the transient receptor potential (TRP) superfamily of cation channels can cause endothelium-dependent vasodilation (Birnbauer et al., 1996; Freichel et al., 2001; Vriens et al., 2005; Köhler et al., 2006; Marrelli et al., 2007; Earley et al., 2009), but, because ion channel activity is difficult to study in native endothelial cells, significant

This work was supported by the National Institutes of Health National Heart, Lung, and Blood Institute [Grant R01-HL091905] (to S.E.), [Grant R01-HL085887] (to M.S.T.).

Parts of these data were presented in poster sessions at Experimental Biology 2011; 2011 Apr 9–13; Washington DC.

Article, publication date, and citation information can be found at <http://molpharm.aspetjournals.org>.

<http://dx.doi.org/10.1124/mol.112.078584>.

[S] The online version of this article (available at <http://molpharm.aspetjournals.org>) contains supplemental material.

**ABBREVIATIONS:** TRP, transient receptor potential; TIRFM, total internal reflection fluorescence microscopy; TRPV, transient receptor potential vanilloid; GSK1016790A, *N*-((1*S*)-1-[[4-((2*S*)-2-[[2,4-dichlorophenyl)sulfonyl]amino]-3-hydroxypropanoyl)-1-piperazinyl]carbonyl]-3-methylbutyl)-1-benzothio-*phene*-2-carboxamide; ROI, region of interest; RT, reverse transcription; PCR, polymerase chain reaction; CPA, cyclopiazonic acid; 4 $\alpha$ -PDD, 4 $\alpha$ -phorbol 12,13-didecanoate; HC-067047, 2-methyl-1-[3-(4-morpholinyl)propyl]-5-phenyl-*N*-[3-(trifluoromethyl)phenyl]-1*H*-pyrrole-3-carboxamide; 11,12-EET, 11,12-epoxyeicosatrienoic acid.

questions regarding the molecular identities and regulation of these channels remain unresolved.

Patch-clamp electrophysiology is routinely used to study ion channel activity. This methodology yields invaluable insight into channel biophysics and pharmacology but also presents significant limitations. In the on-cell and inside-out patch-clamp configurations, channel activity can only be recorded from the small portion of the cell membrane present under the patch pipette. Furthermore, the on-cell configuration does not allow membrane voltage clamp. The traditional whole-cell configuration disrupts intracellular signaling pathways when the cell membrane is ruptured, and cells are dialyzed with the patch pipette solution. In addition to these inherent limitations, further impediments are presented by the morphology of native endothelial cells. Obtaining and maintaining gigohm seals with these small, extremely flat cells is exceedingly difficult, and progress tends to be deliberate. Therefore, a goal of the current study was to develop a robust, efficient method that allows ion channel activity in endothelial cells to be studied under near-physiological conditions. Demuro and Parker (2005) described a method that can be adopted for this purpose using total internal reflection fluorescence microscopy (TIRFM) to record the unitary activity of  $\text{Ca}^{2+}$ -permeable ion channels expressed in *Xenopus laevis* oocytes. In TIRFM, a low-energy evanescent field of illumination is created when incident light is angled such that all of the light is reflected away from the sample (Demuro and Parker, 2005). The wavelength of the evanescent field is equal to that of the incident light but only penetrates the cell surface to a depth of  $\sim 100$  nm to illuminate fluorophores at or near the cell surface (Demuro and Parker, 2005). When cells are loaded with fluorescent  $\text{Ca}^{2+}$  indicator dyes, such as Fluo 4-AM,  $\text{Ca}^{2+}$  microdomains at the cell surface can be imaged (Demuro and Parker, 2005). This technique has significant throughput advantages over conventional patch-clamp methods because it allows for simultaneous recording of all events that occur on the bottom surface of the cell (Demuro and Parker, 2006; Parker and Smith, 2010). In addition, the optical method is less invasive than conventional voltage clamp methods and leaves the intracellular environment undisturbed.

For the current study, we adapted the TIRFM technique to record  $\text{Ca}^{2+}$  influx channel activity in primary human microvascular endothelial cells. In addition, we developed novel software (LC\_Pro, an ImageJ plug-in) for unbiased, automated detection and analysis of endothelial cell  $\text{Ca}^{2+}$  signals. Findings presented here demonstrate that the combination of TIRFM and  $\text{Ca}^{2+}$  signal autodetection with LC\_Pro software is ideal for recording the activity of  $\text{Ca}^{2+}$ -permeable ion channels in endothelial cells. We report novel insight into regulation of TRPV4 channels by the small molecule agonist *N*-((1*S*)-1-[[4-((2*S*)-2-[[2,4-dichlorophenyl]sulfonyl]amino)-3-hydroxypropanoyl]-1-piperazinyl]carbonyl]-3-methylbutyl)-1-benzothiophene-2-carboxamide (GSK1016790A) gained from this method. These findings demonstrate that this methodology represents a significant improvement over the techniques currently used to study ion channel activity in primary cells.

## Materials and Methods

**Cell Culture.** Primary human microvascular endothelial cells from neonate dermis (Cell Systems, Kirkland, WA), passages 3 to 4,

were used in these experiments. Cells were cultured in CSC Complete Medium (Cell Systems) supplemented with 10 ml of Culture-Boost (Cell Systems) and 1 ml of Bac-Off (Cell Systems). Cells were incubated at 37°C and 6%  $\text{CO}_2$ , medium was changed every 2 to 3 days, and cells were subcultured when confluent using 0.05% trypsin-EDTA (Invitrogen). Initial resurrection of cells from stocks frozen in liquid nitrogen required coating of the culture flask with Attachment Factor (Cell Systems) before addition of medium and cells. Before experiments, cells were trypsinized and plated ( $9 \times 10^3$  cells/ml) on 35-mm Mattek dishes (14-mm microwell; Thermo Fisher Scientific, Waltham, MA). Cells were incubated overnight at 37°C and 6%  $\text{CO}_2$ .

**Total Internal Reflection Fluorescence Microscopy.** TIRFM recordings (3-ms exposure time) were acquired using a through-the-lens total internal reflection fluorescence system built around an inverted Olympus IX-70 microscope equipped with an Olympus plan apochromatic 60 $\times$  oil immersion lens (numerical aperture = 1.45) and an Andor iXON charge-coupled device camera. Cells were loaded with Fluo 4-AM (4  $\mu\text{M}$ ) for 20 min at 37°C and 6%  $\text{CO}_2$  in the dark. Cells were washed with and imaged in a physiologic HEPES-buffered solution: 2.5 mM  $\text{CaCl}_2$ , 146 mM NaCl, 4.7 mM KCl, 0.6 mM  $\text{MgSO}_4$ , 0.15 mM  $\text{NaHPO}_4$ , 0.1 mM ascorbic acid, 8 mM glucose, and 10 mM HEPES, pH 7.4. All experiments were performed at room temperature (22–25°C). Each recording was 1000 frames and  $\sim 20$  to 40 s long.

**LC\_Pro Data Analysis.** All data used in analyses were derived directly from the original TIRFM recordings. Recordings were processed using a custom algorithm implemented as a plug-in (LC\_Pro) for ImageJ software specifically designed to 1) detect statistically significant fluorescent signals within background noise, 2) automatically define circular regions of interest (ROIs) (15-pixel diameter) centered at active sites containing statistically significant fluorescent signals, and 3) calculate mean fluorescence intensities within ROIs to determine specific event parameters. Eight-bit gray scale TIFF image sequences are input into LC\_Pro/ImageJ, initially specifying the ROI size (15 pixels) and the frame rate of the input video, and event statistics are generated as the final output, according to the program flow chart outlined in Francis et al. (2012). In brief, image processing was performed through a series of steps: normalization of 8-bit gray scale image stacks to 0.01% saturated pixels, generation of a background frame from a minimum intensity projection of the image sequence, subtraction of the background frame from the original image sequence, and subtraction of a mean intensity projection of the sequence from the background-subtracted image sequence. The resulting image sequence is then divided by the time-dependent S.D. of the background-subtracted image sequence. The ImageJ Particle Analyzer Java class was then used to assign best-fit ellipses at the center of each event. During event processing, the mean intensity within each ROI (ellipse) was calculated using a modified version of the multimeasure plug-in for ImageJ. Events are defined as fluorescent signals that meet several criteria: 1) a spatial restriction of  $\geq 12.56$  pixels per frame, 2) a temporal restriction of  $\geq 2$  frames, and 3) a signal that falls within  $P < 0.01$  for Gaussian variation. The statistical rigor underlying these stringent criteria for event classification allow for substantially high signal/noise discrimination of fluorescent signals. ROI processing follows, where location ( $x,y$ ), spatial spread, amplitude, duration, attack time, and decay time were then calculated for each event. LC\_Pro was customized for our study by the addition of a step in the program flow before the calculation of event duration (during ROI processing) in which the left and right side differences between peak and baseline fluorescence ( $F$ ) were calculated and expressed as  $\Delta F$ . Duration is expressed as the time interval at 50% maximum peak fluorescence. Spatial spread is calculated as the area of the maximum best-fit ellipse at 95% of the peak fluorescence of an event. The LC\_Pro plug-in for ImageJ can be downloaded from the ImageJ Web site <http://rsbweb.nih.gov/ij/plugins/lc-pro/index.html>.

**RNA Isolation and RT-PCR.** Total RNA was extracted from endothelial cells (RNeasy Protect Mini Kit; QIAGEN, Valencia, CA) and first-strand cDNA was synthesized using an Omniscript Reverse Transcriptase kit (QIAGEN). PCR was performed using primer sets specific for TRPV4 (Qiagen), yielding a product of 149 base pairs. PCR products were resolved on 2% agarose gels. PCRs always included a template-free negative control. The PCR product was sequenced to confirm its identity.

**Immunocytochemistry.** Immunocytochemical analysis was used to confirm expression of TRPV4 in primary human microvascular endothelial cells. Cells were fixed with 4% formaldehyde for 10 min, permeabilized with methanol ( $-80^{\circ}\text{C}$ ), blocked with 2% bovine serum albumin (in phosphate-buffered saline), and incubated with a primary rabbit monoclonal antibody specific to TRPV4 (1:250; Alomone Labs, Jerusalem, Israel) overnight at  $4^{\circ}\text{C}$ . Cells were washed and incubated with a fluorescent secondary antibody (goat anti-rabbit) conjugated with a Texas Red fluorophore (1:1000; Santa Cruz Biotechnology, Inc., Santa Cruz, CA) for 2 h at room temperature in the dark. Fluorescence images for immunocytochemistry were obtained using a FluoView 1000 laser-scanning confocal microscope (Olympus) and a  $60\times$  oil immersion objective (numerical aperture = 1.4) with the pinhole diameter set for 1 Airy unit. Excitation of Texas Red was by illumination with the 543-nm line set at 74% transmission, and emission was collected using a variable band-pass filter set to 555 to 655 nm. Excitation of 4,6-diamidino-2-phenylindole was by illumination with the 405-nm line set at 0.1% transmission, and emission was collected using a variable band-pass filter set at 475 to 575 nm. All images were acquired at  $1024 \times 1024$  pixels at  $4.0 \mu\text{s}/\text{pixel}$  and were analyzed in ImageJ (version 1.44b).

**Statistics.** All data are means  $\pm$  S.E. Values of  $n$  refer to the number of cells for each experiment. Statistical tests used for each data set are as follows. One-way analysis of variance was used to test for differences in whole-cell event frequency between treatments with removal of  $\text{Ca}^{2+}$  and with cyclopiazonic acid (CPA); where significant, individual groups were compared using a Student-Newman-Keuls post hoc test (Fig. 1b). Unpaired  $t$  tests were used to determine whole-cell frequency differences with addition of  $4\alpha$ -PDD (Fig. 2e). Two-way analysis of variance was used to test for differences in whole-cell frequency differences between treatments in both the ruthenium red and 2-methyl-1-[3-(4-morpholinyl)propyl]-5-phenyl- $N$ -[3-(trifluoromethyl)phenyl]-1 $H$ -pyrrole-3-carboxamide (HC-067047) experiments as well as the detection method comparison experiments, in which significant, individual groups were compared using a Student-Newman-Keuls post hoc test (Figs. 2, f and g, and 5a). Paired  $t$  tests were used to test for differences in the quantity of events and event sites before and after treatment with GSK1016790A (Fig. 4b). For comparison of non-Gaussian distributed data, a Mann-Whitney rank sum test was used to determine significant differences (Table 1). A level of  $P \leq 0.05$  was accepted as statistically significant for all experiments. Histograms were constructed and fit using OriginPro version 8.5, and SigmaPlot version 11.0 was used to make the figures. The concentration-response curve

(Fig. 2d) was constructed by fitting data to a four-parameter logistic equation (SigmaPlot version 11.0).

## Results

**Novel Subcellular  $\text{Ca}^{2+}$  Influx Events in Primary Human Microvascular Endothelial Cells.** Localized, transient increases in fluorescence were observed at the surface of endothelial cells loaded with Fluo 4-AM and imaged using TIRFM (Movie 1; Fig. 1a; Supplemental Fig. 1). Recordings were analyzed using LC\_Pro to automatically identify subcellular regions with statistically significant changes in surface fluorescence, and the location, amplitude ( $\Delta F = \text{local current peak F} - \text{local current minimum F}$ ), spatial spread, duration, attack time (duration from 50% F to local peak F), and decay time (duration from local peak F to 50% F) of each event were determined. A noise threshold filter ( $\Delta F \leq 0.1$ ) was established on the basis of a common peak observed in event amplitude histograms under all recording conditions. Whole-cell event frequency (Hertz) was calculated as total events per cell per second. Under basal conditions, events had a mean amplitude ( $\Delta F$ ) of  $0.39 \pm 0.01$ , attack time of  $0.88 \pm 0.06$  s, decay time of  $0.99 \pm 0.07$  s, duration of  $2.67 \pm 0.13$  s, whole-cell event frequency of  $0.11 \pm 0.02$  Hz, and spatial spread of  $6.26 \pm 2.01 \mu\text{m}^2$  ( $n = 125$ ). These  $\text{Ca}^{2+}$  signals are longer in duration than those for previously described  $\text{Ca}^{2+}$  events, such as  $\text{Ca}^{2+}$  sparks (Cheng et al., 1993),  $\text{Ca}^{2+}$  sparklets, and  $\text{Ca}^{2+}$  pulsars (Ledoux et al., 2008) (Supplemental Table 1).

To determine whether events recorded from endothelial cells using TIRFM result from  $\text{Ca}^{2+}$  influx from the extracellular solution or from  $\text{Ca}^{2+}$  release from intracellular stores, we disrupted  $\text{Ca}^{2+}$  release from the endoplasmic reticulum with the sarcoplasmic/endoplasmic reticulum  $\text{Ca}^{2+}$  ATPase pump inhibitor CPA ( $10 \mu\text{M}$ ). To demonstrate the efficacy of CPA treatment, global  $\text{Ca}^{2+}$  levels were recorded during administration. As expected, global  $\text{Ca}^{2+}$  levels initially rose upon addition of CPA, and fluorescence returned to basal levels within 15 min (Supplemental Fig. 2). Recordings were obtained from cells pretreated with CPA (15 min) to preclude the possibility of recording store-activated  $\text{Ca}^{2+}$  influx events. CPA had no effect on basal whole-cell event frequency ( $0.12 \pm 0.04$  Hz,  $n = 40$  for control;  $0.15 \pm 0.05$  Hz,  $n = 31$  for CPA) (Fig. 1b). In contrast, we observed that whole-cell event frequency was nearly abolished when  $\text{Ca}^{2+}$  was removed (no added  $\text{Ca}^{2+}$  and 3 mM EGTA) from the extracellular solution ( $0.12 \pm 0.04$  Hz,  $n = 40$  for control;  $0.01 \pm 0.003$  Hz,  $n = 39$  for  $\text{Ca}^{2+}$ -free) (Fig. 1b). These findings indicate that the  $\text{Ca}^{2+}$  signals recorded using TIRFM represent  $\text{Ca}^{2+}$  influx from the extracellular solution.

Histograms for event amplitude, duration, attack time, decay time, and spatial spread were constructed (Fig. 1c). Event amplitudes and durations were broadly distributed, suggesting that the recorded signals result from the activity of multiple types of  $\text{Ca}^{2+}$  influx channels that were active under these conditions.

**Unitary TRPV4 Channel Activity Recorded Using TIRFM.** TRPV4 was identified as a specific molecular target to further evaluate the utility of TIRFM for recording  $\text{Ca}^{2+}$ -permeable channel activity in endothelial cells. TRPV4 was selected because of its biophysical properties, tissue distribu-

TABLE 1

Comparison of basal  $\text{Ca}^{2+}$  influx events versus GSK1016790A-induced events

Amplitude, duration, attack time, decay time, spatial spread, and whole-cell frequency (mean  $\pm$  S.E.) of  $\text{Ca}^{2+}$  influx events recorded from primary endothelial cells under basal conditions (control) or after treatment with the selective TRPV4 agonist GSK1016790A ( $100 \text{ nM}$ ).  $n = 125$  for control;  $n = 59$  for GSK1016790A.

Parameter	Control	GSK1016790A
Amplitude ( $\Delta F$ )	$0.39 \pm 0.01$	$0.22 \pm 0.01^*$
Duration, s	$2.67 \pm 0.13$	$0.52 \pm 0.04^*$
Attack time, s	$0.88 \pm 0.06$	$0.32 \pm 0.02^*$
Decay time, s	$0.99 \pm 0.07$	$0.37 \pm 0.03^*$
Spatial spread, $\mu\text{m}^2$	$6.26 \pm 2.01$	$4.84 \pm 0.82$
Whole-cell frequency, Hz	$0.11 \pm 0.02$	$0.48 \pm 0.05^*$

\*  $P \leq 0.05$  versus control (Mann-Whitney rank sum test).

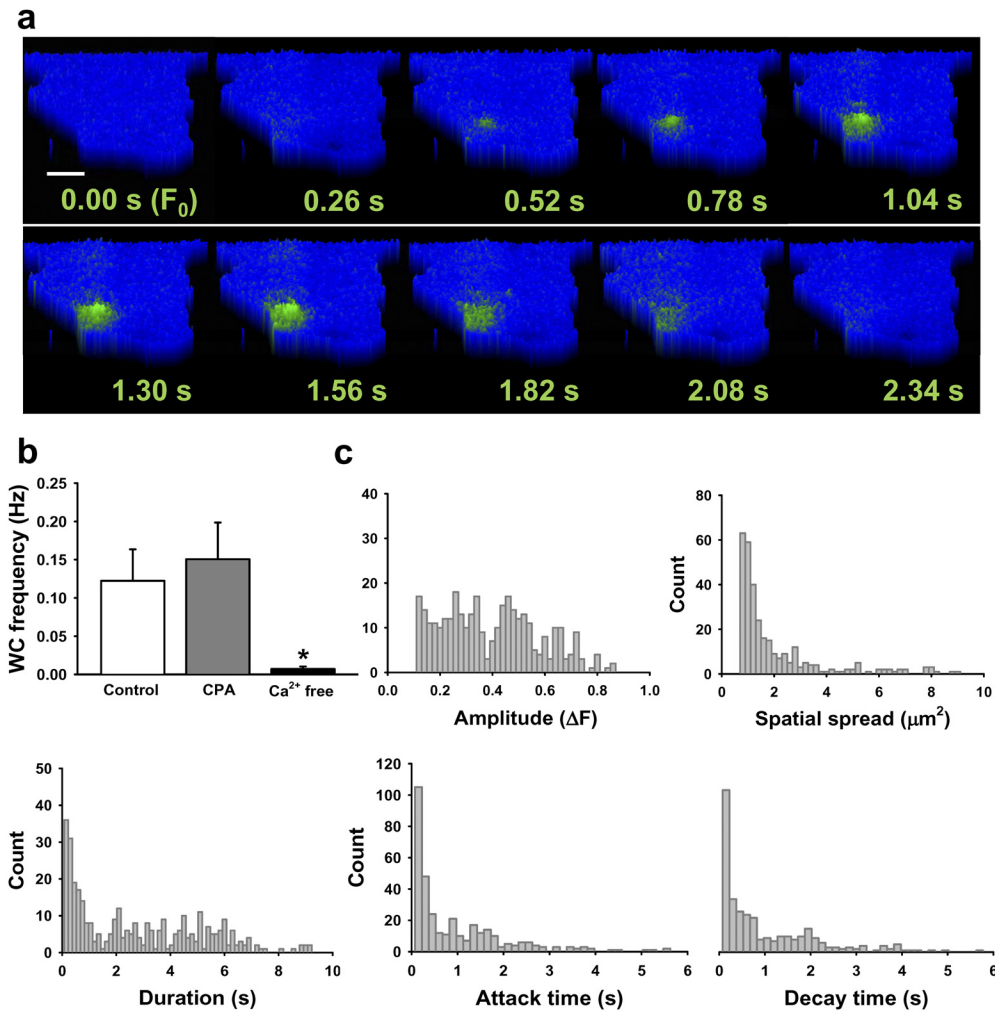


**Fig. 1.** Novel subcellular  $\text{Ca}^{2+}$  influx events in primary human microvascular endothelial cells. **a**, pseudocolor time lapse of a typical  $\text{Ca}^{2+}$  event recorded under control conditions. Scale bar,  $8 \mu\text{m}$ . **b**, mean data showing that depleting intracellular  $\text{Ca}^{2+}$  stores by pretreating with the sarcoplasmic/endoplasmic reticulum  $\text{Ca}^{2+}$  ATPase pump inhibitor CPA ( $10 \mu\text{M}$ ) had no effect on whole-cell (WC) event frequency, whereas removing extracellular  $\text{Ca}^{2+}$  diminished event frequency;  $n = 40$  for control,  $n = 31$  for CPA,  $n = 39$  for  $\text{Ca}^{2+}$ -free. \*,  $P \leq 0.05$  versus control. **c**, histograms of event amplitude, spatial spread, duration, attack time, and decay time. Event amplitudes and duration are randomly distributed, suggesting that multiple types of  $\text{Ca}^{2+}$  channels are active under basal conditions;  $n = 125$  cells.

tion, physiological significance, and available selective pharmacology. TRPV4 channels are slightly selective for  $\text{Ca}^{2+}$  ions ( $P_{\text{Ca}^{2+}}/P_{\text{Na}^{+}} = \sim 9:1$ ), are present in the endothelium of cerebral, mesenteric, and other arterial beds, and are involved in endothelium-dependent vasodilation (Voets et al., 2002; Yang et al., 2006; Marrelli et al., 2007; Brierley et al., 2008). Furthermore, selective pharmacology, including a recently described TRPV4 inhibitor (HC-067047) (Everaerts et al., 2010) and TRPV4 activators (GSK1016790A and  $4\alpha$ -PDD) (Watanabe et al., 2002; Thorneloe et al., 2008), is available.

To establish the presence of TRPV4 in the cells used for this study, RT-PCR was performed using total RNA prepared from primary human microvascular endothelial cells. A band was detected at the expected amplicon length of 149 base pairs, indicating that TRPV4 mRNA is present (Fig. 2a). TRPV4 protein was detected by immunolabeling (Fig. 2b), whereas very little fluorescence was present when the primary antibody was omitted (Fig. 2c), indicating specificity of labeling. TRPV4 protein appears to be uniformly distributed throughout the cell (Fig. 2b).

The effects of the potent TRPV4 agonist GSK1016790A ( $0.1 \text{ nM}$ – $1 \mu\text{M}$ ) were recorded using TIRFM. GSK1016790A increased whole-cell event frequency in a concentration-dependent manner with a near-maximal response at  $[\text{GSK1016790A}] \geq 100 \text{ nM}$  ( $n = 20$ – $30$  cells at each concentra-

tion) (Movie 2; Fig. 2d). The  $\text{EC}_{50}$  value determined from these data ( $26.9 \text{ nM}$ ) is within 1 order of magnitude of the reported  $\text{EC}_{50}$  value ( $3 \text{ nM}$ ) determined using patch-clamp electrophysiology for TRPV4 activation with GSK1016790A in a human embryonic kidney 293 expression system (Thorneloe et al., 2008). GSK1016790A was used at a concentration of  $100 \text{ nM}$  in all subsequent experiments to achieve maximal stimulation. Cell death, indicated by an irreversible global increase in  $\text{Ca}^{2+}$ , was observed in  $\sim 10\%$  of cells exposed to GSK1016790A at this concentration. Data from cells that died during recording were excluded from analyses. GSK1016790A-induced increases in whole-cell event frequency were abolished with removal of extracellular  $\text{Ca}^{2+}$  [ $0.07 \pm 0.03 \text{ Hz}$ ,  $n = 10$  for control;  $0.01 \pm 0.01 \text{ Hz}$ ,  $n = 20$  for  $\text{Ca}^{2+}$ -free + vehicle; and  $0.002 \pm 0.002 \text{ Hz}$ ,  $n = 16$  for  $\text{Ca}^{2+}$ -free + GSK1016790A ( $100 \text{ nM}$ )], demonstrating that these events result from influx of extracellular  $\text{Ca}^{2+}$ . A second, structurally distinct TRPV4 agonist,  $4\alpha$ -PDD ( $10 \mu\text{M}$ ), also increased whole-cell  $\text{Ca}^{2+}$  event frequency in primary endothelial cells ( $0.05 \pm 0.02 \text{ Hz}$ ,  $n = 13$  for control;  $0.36 \pm 0.10 \text{ Hz}$ ,  $n = 21$  for  $4\alpha$ -PDD) (Fig. 2e). 11,12-Epoxyeicosatrienoic acid (11,12-EET) is a potent vasodilator, activates TRPV4 channels (Watanabe et al., 2003), and is endogenously produced by vascular endothelial cells (Earley et al., 2003). 11,12-EET ( $3 \mu\text{M}$ ) also increased the whole-cell frequency of  $\text{Ca}^{2+}$  events relative to vehicle (1% DMSO) ( $0.01 \pm$

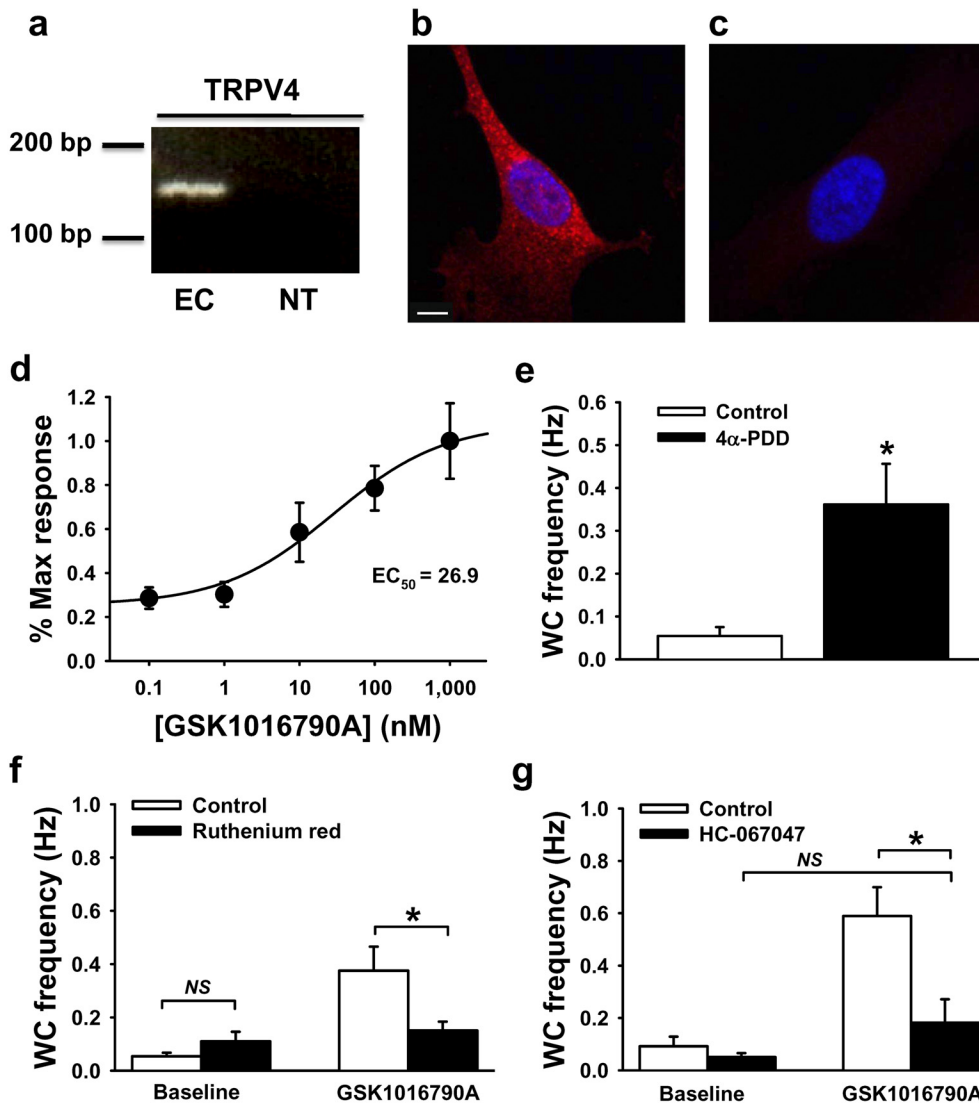


**Fig. 2.** Unitary TRPV4 channel activity recorded using TIRFM. **a**, RT-PCR for TRPV4 using total RNA from primary endothelial cells (EC) compared with a no DNA template control (NT). Data are representative of three experiments. **b**, compressed z-stack images of immunolabeled TRPV4 (red) in primary endothelial cells (b) versus no primary antibody control (c). Nuclei are labeled with 4,6-diamidino-2-phenylindole (blue). Scale bar, 10  $\mu\text{m}$ . Data are representative of three experiments. **d**, concentration-response curve showing the effects of the selective TRPV4 agonist GSK1016790A on whole-cell (WC)  $\text{Ca}^{2+}$  event frequency. **e**, mean data showing that the TRPV4 agonist 4 $\alpha$ -PDD (10  $\mu\text{M}$ ) also increases the whole-cell frequency of  $\text{Ca}^{2+}$  influx events;  $n = 13$  for control and  $n = 21$  for 4 $\alpha$ -PDD. \*,  $P \leq 0.05$  versus control. Pretreatment with the nonspecific TRPV blocker ruthenium red (10  $\mu\text{M}$ ) (f) or the selective TRPV4 inhibitor HC-067047 (500 nM) (g) decreased the stimulation of  $\text{Ca}^{2+}$  event frequency in response to GSK1016790A (100 nM) but had no effect on baseline event frequency. For ruthenium red experiments, under baseline conditions  $n = 29$  for control and  $n = 43$  for ruthenium red; in the presence of GSK1016790A  $n = 17$  for control and  $n = 44$  for ruthenium red. For HC-067047 experiments, under baseline conditions  $n = 26$  for control and  $n = 28$  for HC-067047; in the presence of GSK1016790A  $n = 19$  for control and  $n = 23$  for HC-067047. NS, no statistically significant differences detected. \*,  $P \leq 0.05$  versus control.

0.01 Hz,  $n = 18$  for vehicle;  $0.05 \pm 0.02$  Hz,  $n = 19$  for 11,12-EET) (Supplemental Fig. 3). These findings demonstrate activation of TRPV4-mediated  $\text{Ca}^{2+}$  influx events in endothelial cells by an endogenously produced vasodilator.

The effects of the nonspecific TRPV blocker ruthenium red (10  $\mu\text{M}$ ) and the selective TRPV4 blocker HC-067047 (500 nM) on baseline and GSK1016790A-stimulated (100 nM)  $\text{Ca}^{2+}$  events were examined. Cells were pretreated with physiological solution containing blocker (ruthenium red or HC-067047) or vehicle (distilled water for ruthenium red or dimethyl sulfoxide for HC-067047) for 5 min at room temperature before experimentation. Neither blocker altered the basal  $\text{Ca}^{2+}$  influx event frequency (Fig. 2, f and g). In the absence of ruthenium red, GSK1016790A (100 nM) stimulated an increase in the whole-cell frequency of  $\text{Ca}^{2+}$  events recorded with TIRFM ( $0.05 \pm 0.01$  Hz,  $n = 29$  versus  $0.38 \pm 0.10$  Hz,  $n = 17$ ) (Fig. 2F). A similar response to GSK1016790A (100 nM) was observed in the absence of HC-067047 treatment ( $0.09 \pm 0.04$  Hz,  $n = 26$  versus  $0.59 \pm 0.11$  Hz,  $n = 19$ ) (Fig. 2g). In contrast, GSK1016790A (100 nM) failed to stimulate an increase in event frequency in the presence of ruthenium red ( $0.11 \pm 0.04$  Hz,  $n = 43$  versus  $0.15 \pm 0.03$  Hz,  $n = 44$ ) or HC-067047 ( $0.05 \pm 0.02$  Hz,  $n =$

28 versus  $0.18 \pm 0.09$  Hz,  $n = 23$ ) (Fig. 2, f and g). Taken together, these findings indicate the presence of endogenous, functional TRPV4 channels in human microvascular endothelial cells and demonstrate that the activity of these channels can be recorded and analyzed using TIRFM and LC\_Pro.

**TRPV4-Mediated  $\text{Ca}^{2+}$  Influx Events Are Distinct from Basal Events.**  $\text{Ca}^{2+}$  influx events stimulated by GSK1016790A (100 nM) were further characterized by histogram analysis of event amplitude, spatial spread, duration, attack time, and decay time (Fig. 3, b–d). Of interest, a fit of event amplitudes displays quantal separation (i.e.,  $\Delta F = 0.12, 0.18, 0.23, 0.30$ , and so on), suggesting that these signals represent the activity of an integral number of TRPV4 channels with a unitary  $\Delta F$  value of  $\sim 0.06$  ( $n = 59$ ) (Fig. 3b). Single TRPV4 channel activity ( $\Delta F = 0.06$ ) is apparent in some tracings (Fig. 3c) but could not be resolved from noise in most recordings. Spatial spread, duration, attack, and decay were all narrowly distributed around the respective means (Fig. 3d), consistent with the activation of a single type of ion channel. The mean amplitude of GSK1016790A-induced events was smaller than that of control events and the mean duration, attack, and decay times were significantly shorter (Fig. 3a; Table 1). Spatial spread did not differ between

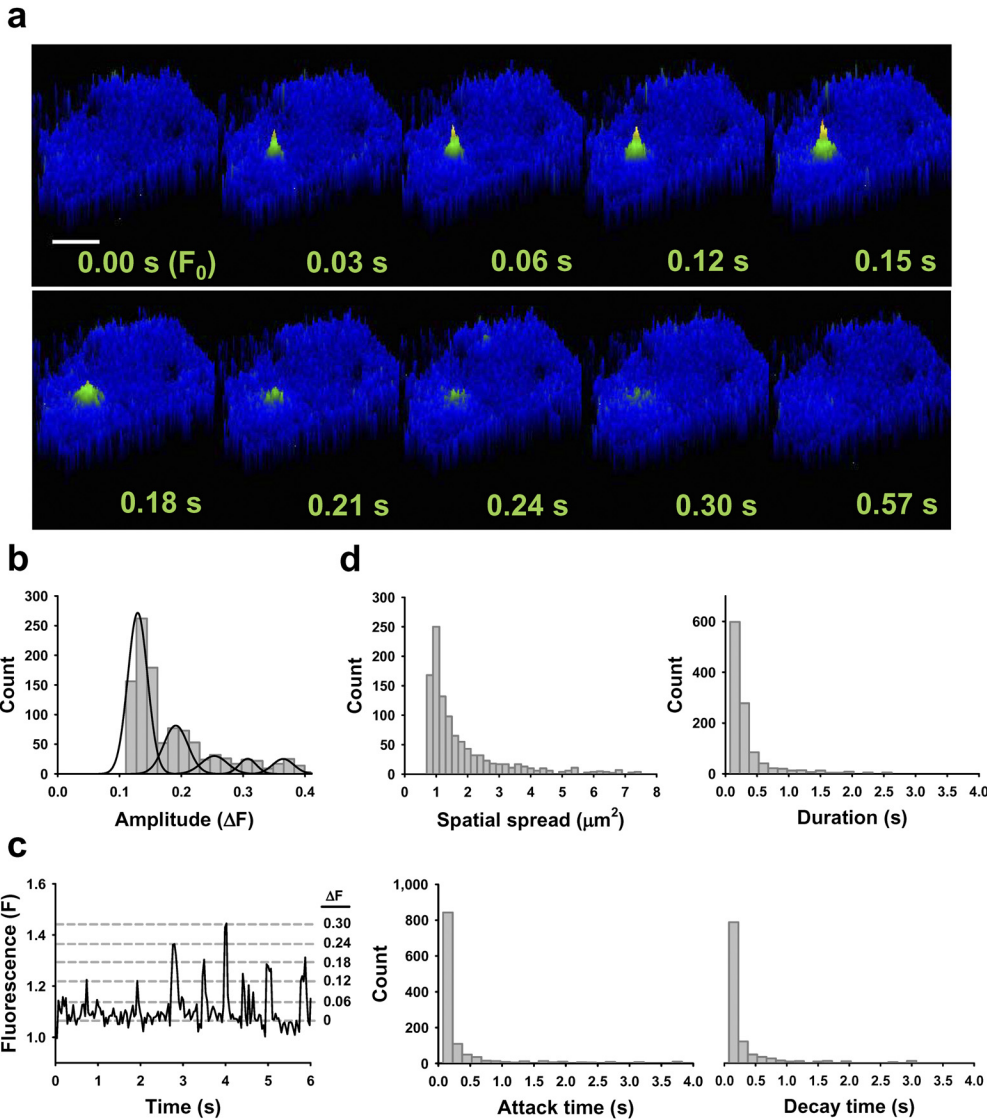


**Fig. 3.** TRPV4-mediated  $\text{Ca}^{2+}$  influx events are distinct from basal events. a, pseudocolor time lapse of a typical  $\text{Ca}^{2+}$  event recorded from a cell treated with GSK1016790A (100 nM). Scale bar, 8  $\mu\text{m}$ . b, histogram analysis of  $\text{Ca}^{2+}$  event amplitude in cells treated with GSK1016790A indicating quantal separation. These event levels can also be observed in a representative plot of fluorescence versus time (c). d, histograms of spatial spread, duration, attack, and decay in cells treated with GSK1016790A.

groups but tended to be smaller for GSK1016790A-induced  $\text{Ca}^{2+}$  influx events (Table 1).

TRPV4-mediated increases in whole-cell event frequency after agonist stimulation could be due to an elevation of the frequency of  $\text{Ca}^{2+}$  influx through basally active channels or could result from the recruitment of new event sites. To distinguish between these possibilities, endothelial cell  $\text{Ca}^{2+}$  events were recorded before and after stimulation with GSK1016790A (100 nM). The total number of events ( $4.78 \pm 1.71$  versus  $12.78 \pm 3.33$ ) and the number of event sites ( $4.22 \pm 1.40$  versus  $8.89 \pm 1.86$ ) per cell was increased after treatment with GSK1016790A (100 nM;  $n = 9$ ) (Fig. 4). Masks of event sites detected by LC\_Pro before and after agonist stimulation were constructed, color-coded, and merged (Fig. 4a). The sites active before (green) versus after (red) agonist administration did not overlap. Of the nine cells that were studied in this experiment, only two had a single site that was active both before and after administration of GSK1016790A. These findings indicate that basal and GSK1016790A-induced  $\text{Ca}^{2+}$  influx events are mediated by distinct populations of ion channels and that quiescent TRPV4 channels are recruited by the agonist. Of interest, although TRPV4 channels appear to be uniformly distributed

throughout the endothelial cell plasma membrane (Fig. 2b), we detected only a few sites of activity using TIRFM when a near-maximal concentration of GSK1016790A was administered (Fig. 4a). These data suggest that much of the channel protein present in endothelial cells is either not present on the plasma membrane or is inactive under these conditions.

## Discussion

The goal of the current study was to develop an efficient method for investigating the activity of  $\text{Ca}^{2+}$ -permeable ion channels in primary endothelial cells. We found that 1) novel, transient, subcellular  $\text{Ca}^{2+}$  influx events can be recorded from primary human endothelial cells and characterized using a combination of TIRFM and LC\_Pro autodetection analysis, 2) the selective TRPV4 agonist GSK1016790A elicits concentration-dependent increases in the whole-cell frequency of  $\text{Ca}^{2+}$  influx events that are attenuated by TRPV4 antagonists and abolished in the absence of extracellular  $\text{Ca}^{2+}$ , 3) the peak amplitude distribution of GSK1016790A-induced  $\text{Ca}^{2+}$  influx events displays quantal separation, suggesting that single-channel activity can be recorded, 4) GSK1016790A-induced  $\text{Ca}^{2+}$  influx events represent newly

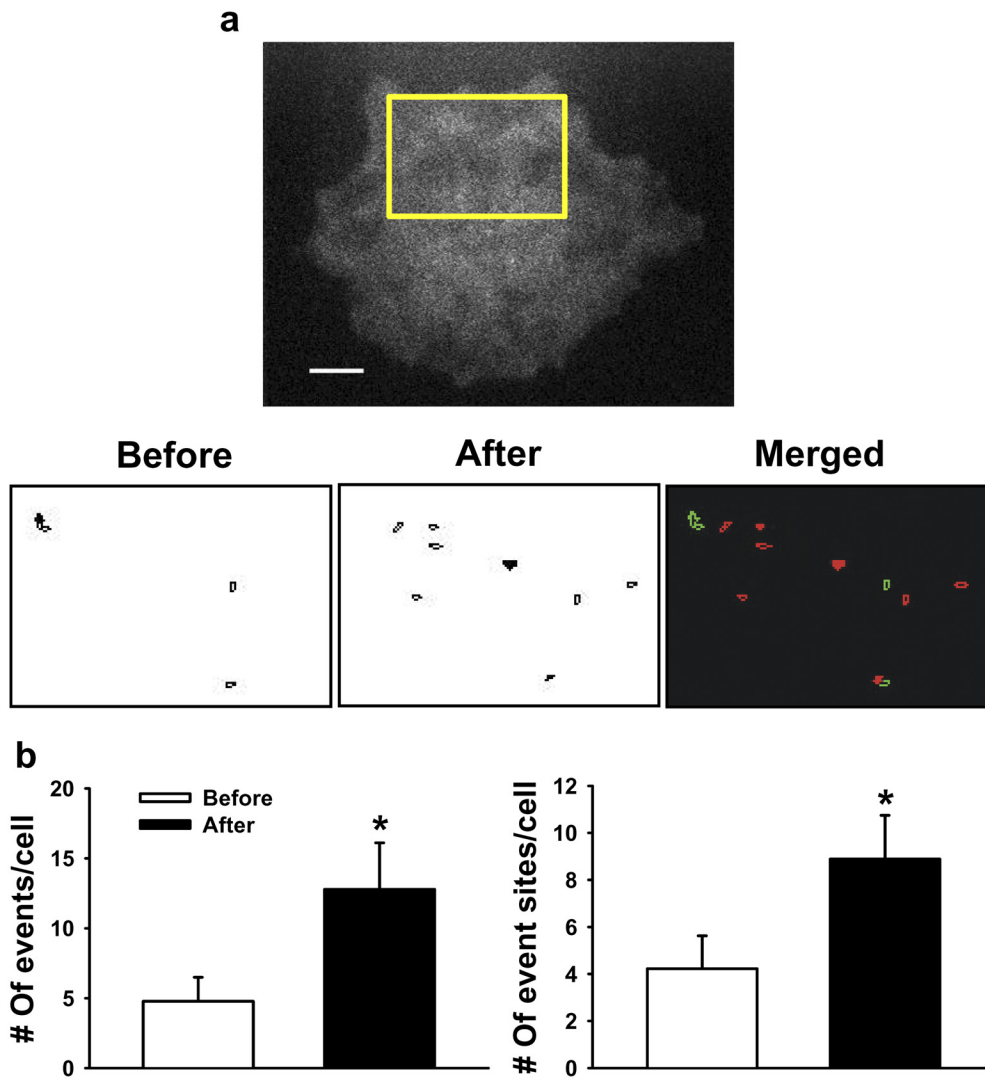


**Fig. 4.** GSK1016790A increases whole-cell event frequency by recruiting new  $\text{Ca}^{2+}$  event sites. **a**, top, TIRFM image of a typical primary endothelial cell.  $\text{Ca}^{2+}$  influx sites detected by LC\_Pro for the indicated region are shown before (left) and after (middle) addition of GSK1016790A (100 nM). The merged pseudocolor image (right) shows events before addition of GSK1016790A in green and after in red. There is no overlap between the event sites. **b**, mean data showing the number of events (left) and the number of event sites (right) per cell before and after addition of GSK1016790A ( $4.78 \pm 1.71$  events/cell before versus  $12.78 \pm 3.33$  events/cell after and  $4.22 \pm 1.40$  sites/cell before versus  $8.89 \pm 1.86$  sites/cell after,  $n = 9$  for each group). \*,  $P \leq 0.05$  versus control.

recruited TRPV4 channels, rather than increased activity of previously established sites, and 5) many of the TRPV4 channels present in endothelial cells remain silent during maximal agonist stimulation. Taken together, these data demonstrate that basal and TRPV4  $\text{Ca}^{2+}$  influx events can be distinguished and characterized using our combined TIRFM/LC\_Pro approach. Moreover, our findings are consistent with the conclusion that GSK1016790A-activated  $\text{Ca}^{2+}$  influx events represent recruitable TRPV4 channel activity in primary endothelial cells. Of importance, these results establish that use of TIRFM with selective pharmacology and LC\_Pro autodetection to record  $\text{Ca}^{2+}$ -permeable ion channel activity in the endothelial cells improves experimental efficiency as well as sensitivity and provides spatial information not provided by conventional patch-clamp techniques.

Changes in intracellular  $[\text{Ca}^{2+}]$  mediate critical functions of the endothelium, including capillary permeability, changes in membrane potential, and production of vasoactive substances. Voltage-clamp electrophysiology is difficult to efficiently apply to native endothelial cells because of their small size and flat morphology; consequently, much remains unknown about the  $\text{Ca}^{2+}$  influx pathways contributing to the regulation of these processes. The current findings demonstrate that TIRFM is a significant improvement over conventional patch-clamp elec-

trophysiology for studying  $\text{Ca}^{2+}$  influx channels in primary endothelial cells. Benefits of TIRFM compared with voltage clamp include higher throughput, the ability to record from cells in an unperturbed state and the capability to simultaneously record the location and biophysical properties of multiple  $\text{Ca}^{2+}$  signals from each cell. In addition, the TIRFM approach provides spatial information that cannot be obtained using traditional patch-clamp electrophysiology. The principle disadvantage of the TIRFM method is the lack of voltage clamp, but this can be compensated for by manipulating the ionic content of the extracellular solution. In addition, the TIRFM technique detects only  $\text{Ca}^{2+}$  influx and does not measure outward currents or currents resulting from the movement of other ions, such as  $\text{Na}^+$  or  $\text{K}^+$ , which contribute to the total activity of nonselective cation channels. Despite these minor limitations, our findings clearly demonstrate the advantages of TIRFM for recording the activity of  $\text{Ca}^{2+}$ -permeable ion channel activity in endothelial cells. Confocal microscopy could also be used to study unitary  $\text{Ca}^{2+}$  influx events in endothelial cells. We selected TIRFM over confocal microscopy for the current study to be consistent with the method used in prior work studying  $\text{Ca}^{2+}$  influx channels (Demuro and Parker, 2005).

The findings of this study demonstrate that distinct types

of  $\text{Ca}^{2+}$  influx events can be recorded from primary endothelial cells using a combination of TIRFM and selective pharmacology. Prior reports suggest that endothelial cells express multiple  $\text{Ca}^{2+}$  influx channels, including several TRP channels (TRPC1, TRPC3, TRPC4, TRPV3, TRPV4, and TRPA1) (Chang et al., 1997; Freichel et al., 2001; Voets et al., 2002; Earley et al., 2009, 2010), the cyclic nucleotide-gated channel A1 (Yao et al., 1999; Wu et al., 2000), and the ATP-sensitive purinergic ligand-gated receptor channel P2X4 (Yamamoto et al., 2000). Consistent with these observations,  $\text{Ca}^{2+}$  influx events recorded from unstimulated primary endothelial cells exhibit a broad distribution of event amplitude and duration, suggesting that these signals arise from more than one type of channel. This study provides the first evidence of spontaneous  $\text{Ca}^{2+}$  channel activity in primary human microvascular endothelial cells. The specific TIRFM properties of one channel, TRPV4, were characterized using selective pharmacological tools.  $\text{Ca}^{2+}$  signals stimulated by a TRPV4 agonist exhibited quantal separation in amplitude, were much shorter in duration ( $\sim 8.5$ -fold), and tended to be larger in area compared with those recorded from unstimulated cells. These data establish a distinctive biophysical "TIRFM fingerprint" for TRPV4 channels in primary endothelial cells. Similar TRPV4  $\text{Ca}^{2+}$  influx events were recently described in intact mouse mesenteric arteries (Sonkusare et al., 2012). With use of a similar approach, other channels can be characterized and identified by their unique properties, enabling rapid identification of  $\text{Ca}^{2+}$ -permeable ion channels in endothelial and other types of cells. Thus, in addition to being a powerful research tool, the TIRFM/LC\_Pro technique can be used in a clinical setting to study native endothelial cells under normal and pathophysiological conditions. For example, endothelial cells isolated from patients via peripheral artery biopsy (Colombo et al., 2002) could be examined by TIRFM/LC\_Pro for changes in endothelial cell  $\text{Ca}^{2+}$  channel activity associated with endothelial dysfunction and cardiovascular disease. The technique may be particularly useful for evaluating the mechanisms of action for drugs designed to improve endothelial function.

The selective agonist GSK1016790A has been extensively used to study the physiological role of TRPV4 channels (Thorneloe et al., 2008; Xu et al., 2009; Gradilone et al., 2010; Jin et al., 2011; Mihara et al., 2011; Ryskamp et al., 2011). However, little is currently known about how GSK1016790A stimulates TRPV4 channel activity. Application of the TIRFM technique revealed new insight into activation of TRPV4 activity by this agonist in primary endothelial cells. We show here for the first time that  $\text{Ca}^{2+}$  influx stimulated by GSK1016790A originates from newly recruited, rather than from previously active, TRPV4 channels. These findings suggest that under the conditions used for this study, TRPV4 channels have a very low open probability. Consistent with this conclusion, neither ruthenium red nor the selective TRPV4 blocker HC-067047 diminished  $\text{Ca}^{2+}$  event frequency under basal conditions, suggesting that events recorded under basal conditions are very unlikely to be mediated by TRPV4 or any other TRPV channel. Of interest, even maximal stimulation of TRPV4 channels with GSK1016790A produced only relatively modest increases in the whole-cell frequency of  $\text{Ca}^{2+}$  influx events and event sites. These findings are consistent with those recently reported by Sonkusare et al. (2012), demonstrating that activation of as few as 3

TRPV4 channels per endothelial cell is sufficient to induce maximal dilation of mouse mesenteric arteries. In addition, the current findings show that much of the TRPV4 channel protein present in primary endothelial cells is inactive during maximal agonist stimulation. The role of "silent" TRPV4 channels in endothelial cells is unclear. It is possible that most of the TRPV4 protein present in primary endothelial cells is not expressed on the plasma membrane and is either nonfunctional or contributes to cellular signaling in a manner that does not involve transport of ions across the plasma membrane. Nonconducting roles for other TRP channels (TRPM1, TRPM6, TRPM7, TRPM2, TRPP1, and TRPP2), hyperpolarization-activated cyclic nucleotide-gated channels, as well as several  $\text{K}^+$  channels (Kv1.3, Kv10.1, and Kv11.1) have been reported (Duncan et al., 1998; Perraud et al., 2001; Runnels et al., 2001; Schlingmann et al., 2002; Huang, 2004; Pardo, 2004; Zhong et al., 2004; Grimm et al., 2006). These studies demonstrate contributions of nonconducting channels to numerous cellular processes including proliferation, mitogen-activated protein kinase signaling, tumor suppression, synaptic facilitation, and channel expression (Duncan et al., 1998; Perraud et al., 2001; Runnels et al., 2001; Schlingmann et al., 2002; Huang, 2004; Pardo, 2004; Zhong et al., 2004; Grimm et al., 2006). It is also possible that conducting TRPV4 channels are present on intracellular membranes, such as the endoplasmic reticulum or Golgi bodies. Additional work is needed to determine the specific role of nonconducting TRPV4 channels in endothelial cells.

In summary, findings presented here demonstrate that TIRFM can be combined with selective pharmacological tools to establish characteristic properties of TRPV4 channels, suggesting that this approach can be used to study the activity of specific  $\text{Ca}^{2+}$ -permeable ion channels. Using this method, we identified new information regarding the activation of TRPV4 by the small molecule agonist GSK1016790A. Furthermore, the findings of this study demonstrate that the novel combination of TIRFM and custom automatic ROI detection software is a significantly improved method for recording and analyzing the activity of  $\text{Ca}^{2+}$ -permeable ion channels in primary endothelial cells. The approach described here may be effective for studying changes in endothelial cell  $\text{Ca}^{2+}$  channel activity during endothelial dysfunction associated with cardiovascular disease.

#### Acknowledgments

We thank Dr. Albert L. Gonzales for technical assistance and critical comments on the manuscript, Dr. Michael M. Tamkun for critical comments on the manuscript, and Dr. Gregory C. Amberg for technical advice.

#### Authorship Contributions

*Participated in research design:* Pitts and Earley.

*Conducted experiments:* Sullivan.

*Contributed new reagents or analytic tools:* Francis and Taylor.

*Performed data analysis:* Sullivan and Earley.

*Wrote or contributed to the writing of the manuscript:* Sullivan and Earley.

#### References

- Birnbaumer L, Zhu X, Jiang M, Boulay G, Peyton M, Vannier B, Brown D, Platano D, Sadeghi H, Stefani E, et al. (1996) On the molecular basis and regulation of cellular capacitance calcium entry: roles for Trp proteins. *Proc Natl Acad Sci USA* 93:15195–15202.
- Brierley SM, Page AJ, Hughes PA, Adam B, Liebrechts T, Cooper NJ, Holtmann G,



- Liedtke W, and Blackshaw LA (2008) Selective role for TRPV4 ion channels in visceral sensory pathways. *Gastroenterology* **134**:2059–2069.
- Chang AS, Chang SM, Garcia RL, and Schilling WP (1997) Concomitant and hormonally regulated expression of trp genes in bovine aortic endothelial cells. *FEBS Lett* **415**:335–340.
- Cheng H, Lederer WJ, and Cannell MB (1993) Calcium sparks: elementary events underlying excitation-contraction coupling in heart muscle. *Science* **262**:740–744.
- Colombo PC, Ashton AW, Celaj S, Talreja A, Banchs JE, Dubois NB, Marinaccio M, Malla S, Lachmann J, Ware JA, et al. (2002) Biopsy coupled to quantitative immunofluorescence: a new method to study the human vascular endothelium. *J Appl Physiol* **92**:1331–1338.
- Demuro A and Parker I (2005) "Optical patch-clamping": single-channel recording by imaging Ca<sup>2+</sup> flux through individual muscle acetylcholine receptor channels. *J Gen Physiol* **126**:179–192.
- Demuro A and Parker I (2006) Imaging single-channel calcium microdomains. *Cell Calcium* **40**:413–422.
- Duncan LM, Deeds J, Hunter J, Shao J, Holmgren LM, Woolf EA, Tepper RI, and Shyjan AW (1998) Down-regulation of the novel gene melastatin correlates with potential for melanoma metastasis. *Cancer Res* **58**:1515–1520.
- Earley S, Gonzales AL, and Crnich R (2009) Endothelium-dependent cerebral artery dilation mediated by TRPA1 and Ca<sup>2+</sup>-activated K<sup>+</sup> channels. *Circ Res* **104**:987–994.
- Earley S, Gonzales AL, and Garcia ZI (2010) A dietary agonist of transient receptor potential cation channel V3 elicits endothelium-dependent vasodilation. *Mol Pharmacol* **77**:612–620.
- Earley S, Pastuszyn A, and Walker BR (2003) Cytochrome p-450 epoxygenase products contribute to attenuated vasoconstriction after chronic hypoxia. *Am J Physiol Heart Circ Physiol* **285**:H127–H136.
- Everaerts W, Zhen X, Ghosh D, Vriens J, Gevaert T, Gilbert JP, Hayward NJ, McNamara CR, Xue F, Moran MM, et al. (2010) Inhibition of the cation channel TRPV4 improves bladder function in mice and rats with cyclophosphamide-induced cystitis. *Proc Natl Acad Sci USA* **107**:19084–19089.
- Francis M, Qian X, Charbel C, Ledoux J, Parker JC, and Taylor MS (2012) Automated region of interest analysis of dynamic Ca<sup>2+</sup> signals in image sequences. *Am J Physiol Cell Physiol* <http://dx.doi.org/10.1152/ajpcell.00016.2012>.
- Freichel M, Suh SH, Pfeifer A, Schweig U, Trost C, Weissgerber P, Biel M, Philipp S, Freise D, Droogmans G, et al. (2001) Lack of an endothelial store-operated Ca<sup>2+</sup> current impairs agonist-dependent vasorelaxation in TRP4<sup>-/-</sup> mice. *Nat Cell Biol* **3**:121–127.
- Gradilone SA, Masyuk TV, Huang BQ, Banales JM, Lehmann GL, Radtke BN, Stroope A, Masyuk AI, Splinter PL, and LaRusso NF (2010) Activation of TRPV4 reduces the hyperproliferative phenotype of cystic cholangiocytes from an animal model of ARPKD. *Gastroenterology* **139**:304.e2–314.e2.
- Grimm DH, Karihaloo A, Cai Y, Somlo S, Cantley LG, and Caplan MJ (2006) Polycystin-2 regulates proliferation and branching morphogenesis in kidney epithelial cells. *J Biol Chem* **281**:137–144.
- Huang CL (2004) The transient receptor potential superfamily of ion channels. *J Am Soc Nephrol* **15**:1690–1699.
- Jin M, Wu Z, Chen L, Jaimes J, Collins D, Walters ET, and O'Neil RG (2011) Determinants of TRPV4 activity following selective activation by small molecule agonist GSK1016790A. *PLoS One* **6**:e16713.
- Köhler R, Heyken WT, Heinau P, Schubert R, Si H, Kacic M, Busch C, Grdic I, Maier T, and Hoyer J (2006) Evidence for a functional role of endothelial transient receptor potential V4 in shear stress-induced vasodilatation. *Arterioscler Thromb Vasc Biol* **26**:1495–1502.
- Köhler R and Hoyer J (2007) The endothelium-derived hyperpolarizing factor: insights from genetic animal models. *Kidney Int* **72**:145–150.
- Ledoux J, Taylor MS, Bonev AD, Hannah RM, Solodushko V, Shui B, Tallini Y, Kotlikoff MI, and Nelson MT (2008) Functional architecture of inositol 1,4,5-trisphosphate signaling in restricted spaces of myoendothelial projections. *Proc Natl Acad Sci USA* **105**:9627–9632.
- Marrelli SP, O'neil RG, Brown RC, and Bryan RM Jr (2007) PLA2 and TRPV4 channels regulate endothelial calcium in cerebral arteries. *Am J Physiol Heart Circ Physiol* **292**:H1390–H1397.
- Mihara H, Boudaka A, Sugiyama T, Moriyama Y, and Tominaga M (2011) Transient receptor potential vanilloid 4 (TRPV4)-dependent calcium influx and ATP release in mouse oesophageal keratinocytes. *J Physiol* **589**:3471–3482.
- Pardo LA (2004) Voltage-gated potassium channels in cell proliferation. *Physiology (Bethesda)* **19**:285–292.
- Parker I and Smith IF (2010) Recording single-channel activity of inositol trisphosphate receptors in intact cells with a microscope, not a patch clamp. *J Gen Physiol* **136**:119–127.
- Perraud AL, Fleig A, Dunn CA, Bagley LA, Launay P, Schmitz C, Stokes AJ, Zhu Q, Bessman MJ, Penner R, et al. (2001) ADP-ribose gating of the calcium-permeable LTRPC2 channel revealed by Nudix motif homology. *Nature* **411**:595–599.
- Runnels LW, Yue L, and Clapham DE (2001) TRP-PLIK, a bifunctional protein with kinase and ion channel activities. *Science* **291**:1043–1047.
- Ryskamp DA, Witkovsky P, Barabas P, Huang W, Koehler C, Akimov NP, Lee SH, Chauhan S, Xing W, Renteria RC, et al. (2011) The polymodal ion channel transient receptor potential vanilloid 4 modulates calcium flux, spiking rate, and apoptosis of mouse retinal ganglion cells. *J Neurosci* **31**:7089–7101.
- Schlingmann KP, Weber S, Peters M, Niemann Nejsum L, Vitzthum H, Klingel K, Kratz M, Haddad E, Ristoff E, Dinour D, et al. (2002) Hypomagnesemia with secondary hypocalcemia is caused by mutations in TRPM6, a new member of the TRP gene family. *Nat Genet* **31**:166–170.
- Sonkusare SK, Bonev AD, Ledoux J, Liedtke W, Kotlikoff MI, Heppner TJ, Hill-Eubanks DC, and Nelson MT (2012) Elementary Ca<sup>2+</sup> signals through endothelial TRPV4 channels regulate vascular function. *Science* **336**:597–601.
- Taylor MS, Bonev AD, Gross TP, Eckman DM, Brayden JE, Bond CT, Adelman JP, and Nelson MT (2003) Altered expression of small-conductance Ca<sup>2+</sup>-activated K<sup>+</sup> (SK3) channels modulates arterial tone and blood pressure. *Circ Res* **93**:124–131.
- Thorneloe KS, Sulpizio AC, Lin Z, Figueroa DJ, Clouse AK, McCafferty GP, Chendrimada TP, Lashinger ES, Gordon E, Evans L, et al. (2008) N-((1S)-1-((4-(2S)-2-((2,4-dichlorophenyl)sulfonyl)amino)-3-hydroxypropanoyl)-1-piperazinyl)carbonyl)-3-methylbutyl)-1-benzothiophene-2-carboxamide (GSK1016790A), a novel and potent transient receptor potential vanilloid 4 channel agonist induces urinary bladder contraction and hyperactivity: part I. *J Pharmacol Exp Ther* **326**:432–442.
- Vanhoutte PM (2004) Endothelium-dependent hyperpolarizations: the history. *Pharmacol Res* **49**:503–508.
- Voets T, Prenen J, Vriens J, Watanabe H, Janssens A, Wissenbach U, Bödding M, Droogmans G, and Nilius B (2002) Molecular determinants of permeation through the cation channel TRPV4. *J Biol Chem* **277**:33704–33710.
- Vriens J, Owсяnik G, Fisslthaler B, Suzuki M, Janssens A, Voets T, Morisseau C, Hammock BD, Fleming I, Busse R, et al. (2005) Modulation of the Ca<sub>v</sub>2 permeable cation channel TRPV4 by cytochrome P450 epoxygenases in vascular endothelium. *Circ Res* **97**:908–915.
- Watanabe H, Davis JB, Smart D, Jerman JC, Smith GD, Hayes P, Vriens J, Cairns W, Wissenbach U, Prenen J, et al. (2002) Activation of TRPV4 channels (hVRL-2/mTRP12) by phorbol derivatives. *J Biol Chem* **277**:13569–13577.
- Watanabe H, Vriens J, Prenen J, Droogmans G, Voets T, and Nilius B (2003) Anandamide and arachidonic acid use epoxyeicosatrienoic acids to activate TRPV4 channels. *Nature* **424**:434–438.
- Whorton AR, Willis CE, Kent RS, and Young SL (1984) The role of calcium in the regulation of prostacyclin synthesis by porcine aortic endothelial cells. *Lipids* **19**:17–24.
- Wu S, Moore TM, Brough GH, Whitt SR, Chinkers M, Li M, and Stevens T (2000) Cyclic nucleotide-gated channels mediate membrane depolarization following activation of store-operated calcium entry in endothelial cells. *J Biol Chem* **275**:18887–18896.
- Xu X, Gordon E, Lin Z, Lozinskaya IM, Chen Y, and Thorneloe KS (2009) Functional TRPV4 channels and an absence of capsaicin-evoked currents in freshly-isolated, guinea-pig urothelial cells. *Channels (Austin)* **3**:156–160.
- Yamamoto K, Korenaga R, Kamiya A, Qi Z, Sokabe M, and Ando J (2000) P2X<sub>4</sub> receptors mediate ATP-induced calcium influx in human vascular endothelial cells. *Am J Physiol Heart Circ Physiol* **279**:H285–H292.
- Yang XR, Lin MJ, McIntosh LS, and Sham JS (2006) Functional expression of transient receptor potential melastatin- and vanilloid-related channels in pulmonary arterial and aortic smooth muscle. *Am J Physiol Lung Cell Mol Physiol* **290**:L1267–L1276.
- Yao X, Leung PS, Kwan HY, Wong TP, and Fong MW (1999) Rod-type cyclic nucleotide-gated cation channel is expressed in vascular endothelium and vascular smooth muscle cells. *Cardiovasc Res* **41**:282–290.
- Zhong N, Beaumont V, and Zucker RS (2004) Calcium influx through HCN channels does not contribute to cAMP-enhanced transmission. *J Neurophysiol* **92**:644–647.

**Address correspondence to:** Dr. Scott Earley, Department of Biomedical Sciences, Colorado State University, Fort Collins, CO 80523-1680 E-mail: scott.earley@colostate.edu